S. Bair
Mem. ASME.

I. Green
Mem. ASME.

George W. Woodruff
School of Mechanical Engineering,
Georgia Institute of Technology,
Atlanta, GA 30332-0405

B. Bhushan*
Department of Mechanical Engineering,
University of California at Berkeley,
Berkeley, Calif. 94720.
Fellow ASME

Measurements of Asperity Temperatures of a Read/Write Head Slider Bearing in Hard Magnetic Recording Disks

An infrared temperature measurement system was used to measure hot spots in a magnetic head rigid disk interface. The system employed the spectral distribution as well as intensity of sampled radiation to determine both the temperature and effective area of microscopic sources at elevated temperature. Flash temperatures between particulate and thin-film rigid disks and a simulated transparent sapphire slider at various operating conditions were measured.

1 Introduction

In hard disk magnetic storage devices, the read/write head is intended to operate with a separating air film of thickness several times the surface roughness of the disk. Contact occurs during start-up and stop of disk rotation. Isolated contacts may occur during external vibration stimuli (shock loading) of the drive structure. Contact may also be induced by debris particles which disrupt the disk surface. The disk surface temperatures at these contacts are of interest to designers (Bhushan, 1990). A previous program (Bhushan et al., 1985; Gulino et al., 1986) to measure head/tape contact temperatures was successful only in measuring the bulk surface temperature of the tape and not the transient temperature flashes at asperity contacts. In that program, the temperature was found from the measurement of the total radiative power over a range of wavelength (radiation temperature technique) of the target surface and comparison with the black body temperature for the same radiative power. This required that the target spot either fill the detector field of view or be of a known area. The detector field of view was small (120 μm) so that there was a small probability of having a temperature flash occur where it could be detected. If the asperity contact size is much smaller (for magnetic tapes, it was found to be typically 6–8 μm (Bhushan, 1984, 1985)) than the field of view, then the measured temperature, which is averaged over the field of view, is much smaller than the actual flash temperature.

A differing approach similar to Weichart and Schonert (1978) was taken in this work. Temperatures were found from the spectral distribution (distribution temperature technique) of the radiation emitted. The ratio of emissive powers at two different wavelengths were measured. The maximum temperature in the field of view was then obtained from the power ratios at these two wavelengths. The size of the source need not be known beforehand but may be calculated from the emissive power measured. Therefore the field of view can be made large enough so that any temperature flashes from the area of interest (larger than the resolution limit) can be detected.

This paper presents the distribution temperature technique,

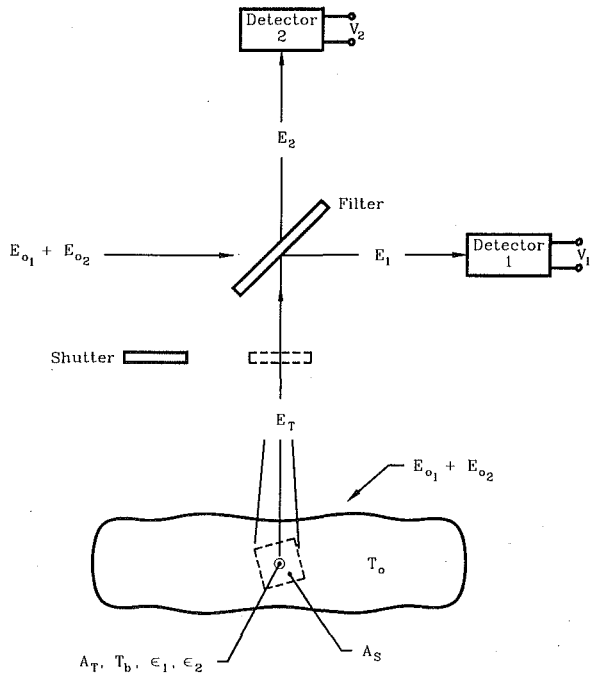

Fig. 1 Schematic representation of the radiation paths

*On sabbatical leave from IBM Research Division, Almaden Research Center, San Jose, Calif. 95120.

Contributed by the Tribology Division of THE AMERICAN SOCIETY OF MECHANICAL ENGINEERS and presented at the Joint ASME/STLE Tribology Conference, Toronto, Canada, October 7–10. Manuscript received by the Tribology Division January 18, 1990; revised manuscript received July 6, 1990. Paper No. 90-Trib-53. Associate Editor: P. A. Willermet.

experimental apparatus, and measured temperature flashes of various head slider-disk interfaces under various operating conditions.

2 Theory of Spectral Distribution Technique

The radiation paths of the distribution temperature measurement system are represented schematically in Fig. 1. The area of the field of view on the target surface is A_s. The bulk of this surface and the surrounding environment is assumed to be at ambient temperature, T_0. A feature at uniform elevated temperature, T_b, with area, A_T, is located within the field of view. This feature represents a hot spot. The emissivity, ϵ, of the surface is assumed to be a function of wavelength, λ, such that

$$\epsilon = \epsilon_1 \text{ for } \lambda_0 < \lambda < \lambda_1$$
$$\epsilon = \epsilon_2 \text{ for } \lambda_1 < \lambda < \lambda_2$$

The short wavelength and long wavelength emissive powers of the ambient radiation, E_{01} and E_{02}, are defined with similar wavelength dependence as are the reflectivity, ρ_1 and ρ_2, and the transmissivity, τ_1 and τ_2, of the filter. The emissivity and reflectivity of the target surface sum to unity. The total radiative power, E_T, entering the optics when the shutter is open is then

$$E_T = \frac{A_T}{A_S}\left[\epsilon_1 E_{b1} + \epsilon_2 E_{b2} + (1-\epsilon_1)E_{01} + (1-\epsilon_2) E_{02}\right] + \left(1 - \frac{A_T}{A_S}\right)(E_{01} + E_{02}) \quad (1)$$

where E_{bi} is the black body emissive power at T_b from λ_{i-1} to λ_i (i = 1,2).

The filter does not transmit at short wavelength (τ_1 = 0) and does not reflect at long wavelength (ρ_2 = 0). The power received at detector 1 reduces to

$$E_1 = \frac{A_T}{A_S}\rho_1 \epsilon_1 (E_{b_1} - E_{0_1}) + \rho_1 E_{0_1} + \tau_2 E_{0_2} \quad (2a)$$

and at detector 2

$$E_2 = \frac{A_T}{A_S}\tau_2 \epsilon_2 (E_{b2} - E_{02}) + \tau_2 E_{02} + \rho_1 E_{01} \quad (2b)$$

If the shutter, which is at T_0, is closed the detectors receive

$$E_{1s} = E_{2s} = \rho_1 E_{01} + \tau_2 E_{02} \quad (3)$$

The differences between radiative powers detected with shutter opened and closed are

$$E_1 - E_{1s} = \rho_1 \epsilon_1 \frac{A_T}{A_S}(E_{b1} - E_{01})$$
$$E_2 - E_{2s} = \tau_2 \epsilon_2 \frac{A_T}{A_S}(E_{b2} - E_{02}) \quad (4a)$$

It should be noted that E_{1s} and E_{2s} are also the detected radiation powers from a surface at T_0 before any hot spot appears. To eliminate the areas, take the ratio

$$\frac{E_2 - E_{2s}}{E_1 - E_{1s}} = \frac{\tau_2 \epsilon_2}{\rho_1 \epsilon_1}\left(\frac{E_{b2} - E_{02}}{E_{b1} - E_{01}}\right) = R^* \quad (4b)$$

Over a domain of temperature T_b there is a unique R^* for each T_b. This is the basis for the temperature measurement technique described here which does not require advance knowledge of the target size, A_T. In addition, R^* is not sensitive to other effects which attenuate the detector signals equally (e.g., response time). However, the analysis of real detector signals is complicated by the fact that the detector response is wavelength dependent.

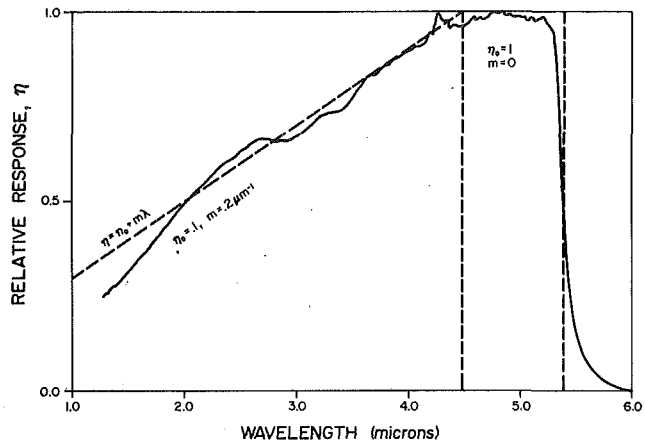

Fig. 2 Relative detector response

The detector voltage, V, can be described by

$$\frac{dV}{d\lambda} = k\eta \frac{dE}{d\lambda}, \quad \eta(\lambda) = \eta_0 + m\lambda \quad (5)$$

where k is sensitivity and η is the relative spectral response as shown in Fig. 2 for the detectors used here. The monochromatic emissive power is given by Planck's law

$$\frac{\partial E_b}{\partial \lambda} = C_1 \lambda^{-5}[\exp(C_2/\lambda T_b) - 1]^{-1}$$

which for this temperature range is normally approximated by

$$\frac{\partial E_b}{\partial \lambda} \simeq C_1 \lambda^{-5} \exp(-C_2/\lambda T_b)$$

where C_1 and C_2 are constants. The unfiltered detector response to a black body is obtained by integration of equation (5)

$$V_{b_i} = kC_1 \int_{\lambda_{i-1}}^{\lambda_i} (\eta_0 + m\lambda)\, \lambda^{-5} \exp(-C_2/\lambda T_b) d\lambda$$

which gives

$$V_{bi} = \bar{k} C_1 e^{-A/\lambda}\left[\eta_0\left[\frac{1}{A\lambda^3} + \frac{3}{A^2\lambda^2} + \frac{6}{A^3\lambda} + \frac{6}{A^4}\right] + m\left[\frac{1}{A\lambda^2} + \frac{2}{A^2\lambda} + \frac{2}{A^3}\right]\right]_{\lambda_{i-1}}^{\lambda_i} \quad (6)$$

where $A = C_2/T_b$. V_{0i} is obtained by replacing T_b by T_0 in equation (6).

The expression which is similar to equation (4) for the difference in detector signal for open versus closed shutter is the same as for the signal rise at the appearance of a hot spot, and is

$$V_1 - V_{1s} = \rho_1 \epsilon_1 \frac{A_T}{A_S}(V_{b1} - V_{01}) \quad (7a)$$
$$V_2 - V_{2s} = \tau_2 \epsilon_2 \frac{A_T}{A_S}(V_{b2} - V_{02})$$

We define R as

$$R = (V_2 - V_{2s})/(V_1 - V_{1s}) \quad (7b)$$

which is independent of both sensitivity, k, and spot size, A_T. The ratio R monotonically decreases from 2 to 0.4 for temperatures ranging from 50 to 600°C. However, we would rather have an expression for T_b as a function of R. An approximation of the form

$$T_b \simeq A_0 \ln(a_1 + a_2 R + a_3 R^2) \quad (8)$$

for equation (4) was found numerically which gives T_b as a

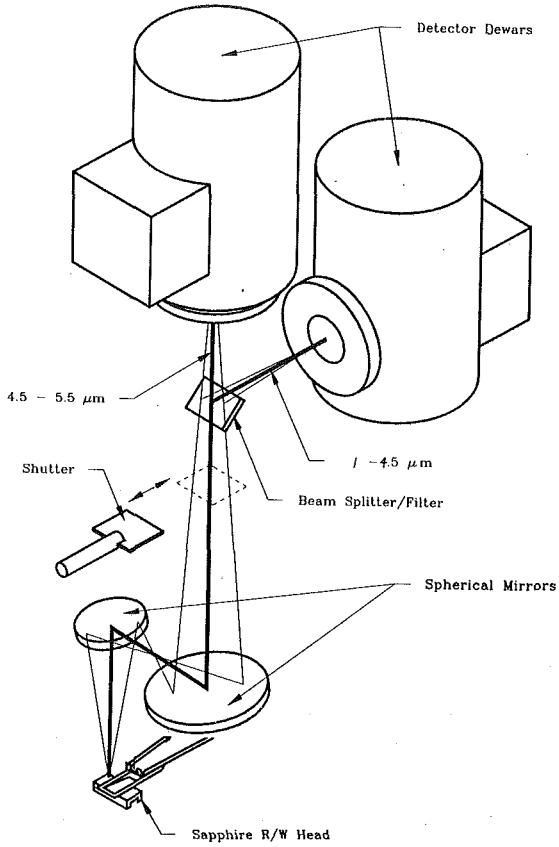

Fig. 3 Optics

function of R within 10°C in the range 50°C to 500°C, where A_0, a_1, a_2, and a_3 are constants. Once T_b is known, the spot area can be found from

$$A_T = \frac{A_s}{\rho_1 \epsilon_1} \frac{(V_1 - V_{1s})}{(V_{b1} - V_{01})} \tag{9}$$

or the similar relation for signal from detector 2 where V_b is obtained from equation (6).

3 Experimental Apparatus

3.1 Optical System. Radiation from the entire apparent contact area was accepted through an aperture and divided into two channels by an edge filter used as a beam splitter. The two channels measured the radiative powers at two different wavelength ranges: 1 to 4.5 μm, and 4.5 to 5.5 μm. The ratio of the signals gave the spectral distribution of radiant power independent of overall signal level and was a sensitive measurement of the temperature of the hottest regions of the field of view.

In the system shown in Fig. 1 only a small portion of the total emissive power from A_T reaches the detector due to the small detector element size and the long working distance (which yields a small solid angle of acceptance). A large improvement in signal magnitude was obtained by building a reflecting system specifically for this application. The final system is shown in Fig. 3, using two first surface spherical mirrors to give a magnification of approximately one, an entrance pupil diameter of about 10 mm and a working distance of about 60 mm. The uniform field of view is 1.2 mm across.

A long pass filter with 4.5 μm cut-off was used as a beam splitter as shown in Fig. 3. The split beams were individually measured with two single-element detector dewars (cooled using LN_2) with integral preamplifier electronics. These detectors operate from 1 to 5.5 μm wavelength (λ_0 and λ_2, respectively) and have a 1 mm by 1 mm active element. Instead of installing

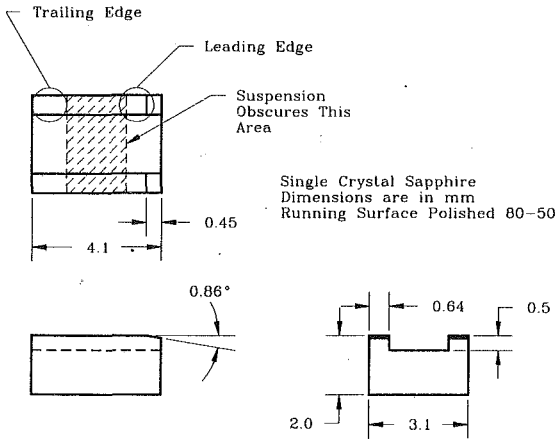

Fig. 4 Simulated R/W head

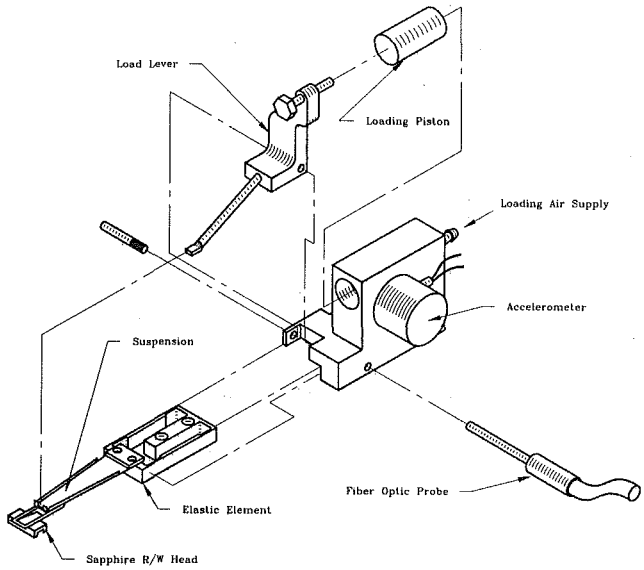

Fig. 5 Exploded view of the R/W head suspension system

internal cold apertures to block excessive background radiation, concave mirrors with a central hole were mounted on the window of each detector. In this manner, outside of the aperture of the concave mirror each element sees its own image at LN_2 temperature. The manufacturer states a 3db frequency response of 150 kHz for the detector dewars. It was found to be beneficial to increase the preamplifier gain by increasing the feed-back resistance by a factor of eight. This should have somewhat reduced the frequency response. A chopper was placed between the detector and a temperature source. Exposure times of 42, 32, 24, 18, and 8 μs were applied. Little signal attenuation was observed for pulses longer than 18 μs. Reported hot spot durations of less than 18 μs are slightly underestimated and areas have been corrected for this effect. The shutter allowed quick measurement of ambient radiation. It is a strength of this technique that if the frequency response of the two detectors is identical, the ratio of signals and therefore, the measured temperature should be unchanged for signals of frequency content above the detector response limit.

3.2 Disk Drive System. The simulated read/write head slider bearing is shown in Fig. 4. The dimensions are similar to the dimensions of an IBM 3370 slider. The material is single crystal sapphire-chosen for wear resistance and infrared transmission. A 130 mm disk drive (3600 rpm) was used. The head was glued to an IBM 3370 type suspension as shown in Fig. 5. The suspension acting as a spring exerts on the slider a

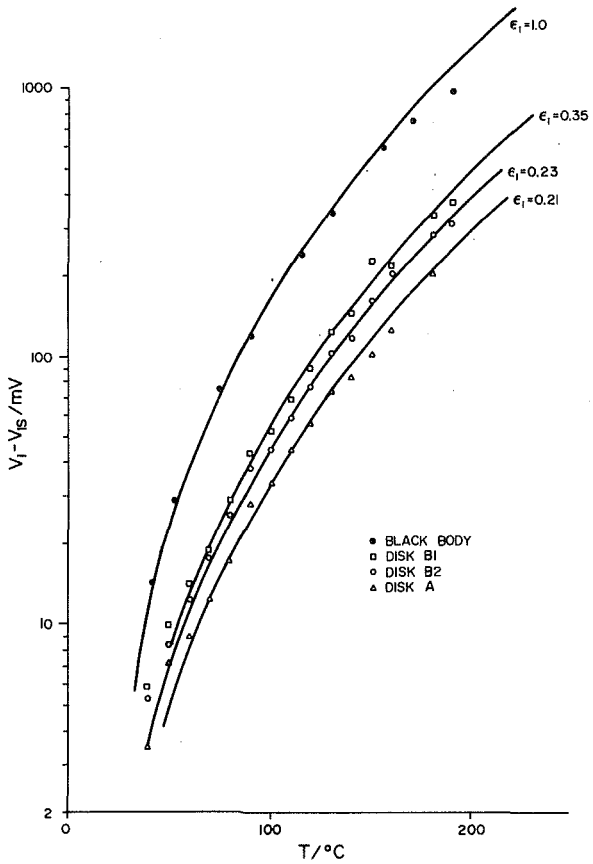

Fig. 6(*a*) System calibration

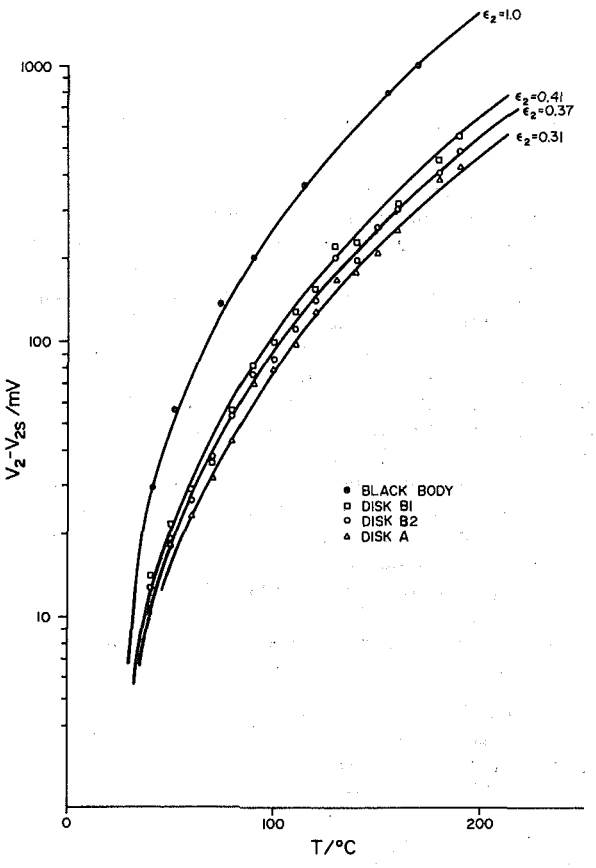

Fig. 6(*b*) System calibration

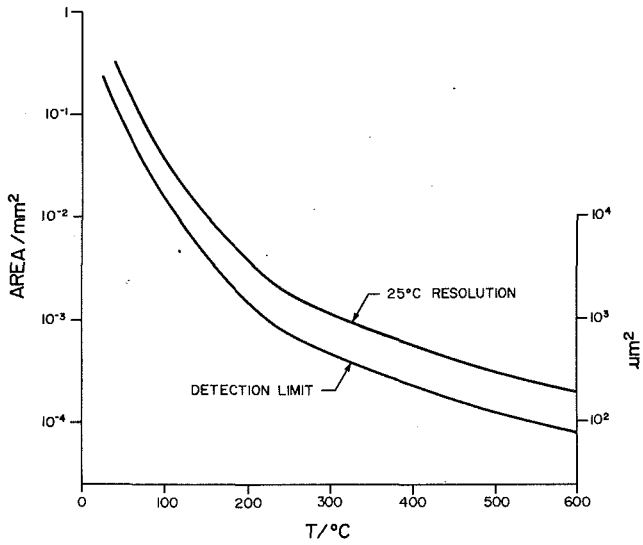

Fig. 7 Minimum target areas for $\epsilon_1 = \epsilon_2 = .3$

nearly constant load of 0.102 N. Additional load may be applied using air pressure against the loading piston shown in the figure. The suspension was mounted to the drive base through an elastic strain element. The elastic strain element will deform in response to the friction force and this deformation is detected by an optical probe in order to measure the friction force. Two elastic elements were fabricated with stiffnesses of 2.2 and 19 N/mm. The element with lowest stiffness vibrated severely when contact occurred between head and disk. Consequently, only the stiffer element was used in the reported experiments. A piezoelectric accelerometer was provided to measure the relative vibration of the suspension assembly.

A polymeric particulate and two thin-film disks were selected for the study. These were same as disks A, B1, and B2 used by Bhushan and Doerner (1989). They are described below:

Disk A— Al-Mg substrate, γ-Fe_2O_3 magnetic particles and load bearing Al_2O_3 particles in a polymer matrix plus 20 to 30 nm thick perfluoropolyether (PFPE) lubricant top coat

Disk B1— Al-Mg substrate, about 10 μm thick Ni-P layer, about 70 nm thick Co-Pt-Ni magnetic layer, about 20 nm thick amorphous carbon overcoat and about 1-4 nm thick PFPE lubricant top coat

Disk B2— Same as B1 except ZrO_2-Y_2O_3 overcoat

The roughness of disks A and B1/B2 were 0.019 μm and 0.010 μm CLA, respectively.

3.3 Infrared System Calibration. A miniature hot stage was fabricated for this program to accept coupons of disk material approximately 1 cm square. A commerical blackbody source was also available. Calibrations were performed by subtracting the detector voltage output resulting from the closed shutter from the output with the shutter open, and either a disk surface or the blackbody in the field of view of the temperature measurement system. Disk samples were calibrated with a 1 mm thick sapphire window resting upon the surface.

It was necessary to adjust the system so that the field of view of the two detectors coincided. This was accomplished by moving a hot wire through the field of view and positioning the detectors so that the signals were coincident. This was done in two orthogonal directions.

The spot size or the area of the field of view was determined. A slit was moved through the field of view between the blackbody source and the optics. As the slit was progressively opened, the peak signal was recorded. This was done in two orthogonal directions. The peak signal increased linearly with slit opening

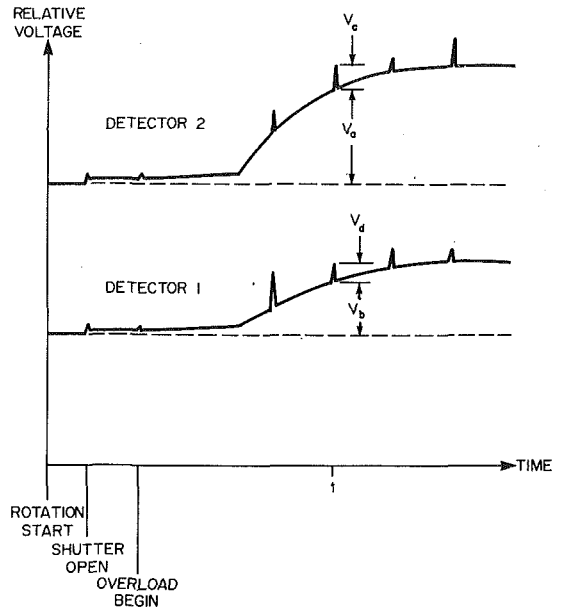

Fig. 8 Detector signals for continuous overload

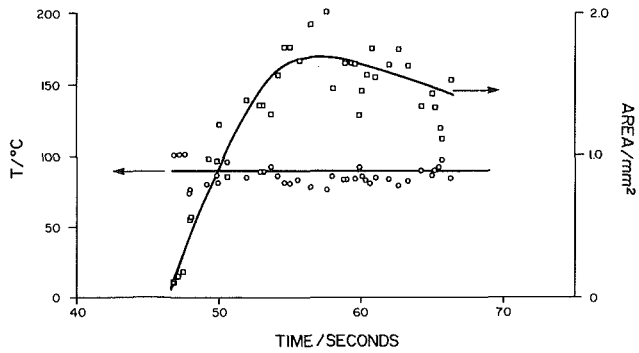

Fig. 9 Background temperature for continuous overloading

until the opening was 1.2 mm. However, the signal continued to increase as the slit was opened to 4 mm. Apparently, this was due to aberrations in the optics. The system detects radiation uniformly from a spot of 1.2 mm by 1.2 mm. When a target fills the field of view (4 mm), the system accepts radiation from the target equivalent to a spot 2 mm by 2 mm of uniform radiation. This is the area, A_s.

Signals were obtained from the blackbody source at various temperatures and were compared to equations (6) and (7*a*) to obtain the detector sensitivity, k, which was found to be the same for both detectors. The fit of equation (6) to the detector response is shown in Fig. 6(*a*) and (*b*) and is excellent. The filter parameters ρ_1, τ_2, and λ_1, were obtained from the filter manufacturer. After obtaining the sensitivity value, k, with the black body, disk surface emissivities, ϵ_1 and ϵ_2, were calculated from detector readings for each of the three hard disk specimens with a sapphire plate in contact with the disk to simulate the presence of the R/W head. The long wavelength emissivity, ϵ_2, was in each case greater than the short wavelength emissivity, ϵ_1. This is apparently due to the presence of the sapphire as when the overlaying sapphire was removed the emissivities were nearly the same. The emissivities may be read from Figs. 6(*a*) and (*b*).

The minimum contact area for a detectable temperature event was estimated based on signal noise and is plotted in Fig. 7. Also shown is the minimum target area for a 25°C temperature resolution based on recorder resolution and equation (8).

Table 1 Hot Spots During Continuous Overload, Disk B1, 1.8 N Load

	Time	Duration	Temperature	Area
	ms	μs	°C	μm²
1.	0.51	26	603	522
2.	0.79	27	536	895
3.	1.12	16	583	1280
4.	1.31	44	377	3313
5.	1.43	33	583	240
6.	1.67	50	486	1050
7.	2.28	36	539	1568
8.	3.07	20	539	890
9.	4.71	26	512	1919
10.	5.17	45	477	1658
11.	5.58	53	411	3082
12.	6.01	42	578	1304
13.	6.82	59	512	790
14.	7.10	21	619	858
15.	8.35	29	496	1608
16.	8.97	47	542	673
17.	9.32	29	404	1722
18.	9.84	29	486	2099
19.	10.27	30	446	2154
20.	10.66	53	496	1608
21.	10.94	24	480	1768
22.	11.33	36	512	677
23.	11.89	77	393	2527
24.	12.62	36	428	3323
25.	13.51	30	527	1456
26.	14.18	29	512	1467
27.	14.51	23	597	761
28.	14.98	62	344	3795
29.	15.37	32	440	1542
30.	16.18	26	619	429
31.	16.39	57	374	2069
32.	16.97	33	534	1903
33.	17.21	21	512	903
34.	19.04	47	446	2154
35.	20.12	45	512	1806
36.	20.66	21	533	1007
37.	21.54	35	344	3795
38.	21.90	32	499	1945
39.	22.46	21	512	790

4 Results and Discussions

4.1 Temperature Measurements. Contact temperatures were measured by locating the field of view of the temperature measurement system over either the leading or the trailing edge of either of the two slider bearings, as shown in Fig. 4. These locations were chosen because the suspension obscures the center 2 mm of the slider bearing.

Initially signals were recorded using a Gould 9000 data acquisition system. This allowed friction force and vibration to be recorded simultaneously with the two detector signals. Maximum sampling rate with this recorder is 0.3 MHz with 8000 samples per channel. All measurements made with a continuous overload were recorded with this device. Due to the long delay in being able to view recorded signals with the Gould recorder all other measurements were recorded on a digital oscilloscope with 2 MHz capability but with only two channels with 2000 samples per channel. Both of the recording systems have disk storage.

Six modes of disk operation were investigated here.

I. Normal flying with 0.1 N normal load
II. Start-up from rest and stopping
III. Continuous overload of 1.8 N
IV. Flying with particulate debris in the path (0.1 N)
V. Flying (0.1 N) after short overload (1.8 N for 0.3s)

No temperature events were recorded for the first two modes on any of the three disks. Approximately 100 start-stop cycles were viewed with the majority of the work being done on disk B1 since its higher emissivity improves the signal magnitude. Hot spots may have occurred of duration or of area too small to be detected.

4.1.1 Continuous Overload. When a load of 1.8 N was

applied to the flying head and was maintained, visible damage occurred to the disk surface after about ten seconds. At this time the detectors began to indicate a slowly rising radiation level which eventually (after 10s) became steady. Imposed on this slow-changing signal were radiation peaks of about 30 μs duration. The temperature associated with the slow changing signal will be called the background temperature. If the radiation peaks are due to hot features of very much smaller area than what produces the background temperature, a hot spot temperature can be calculated from the ratio of these peaks as illustrated in Fig. 8. At time, t, the background temperature is calculated from $R = V_a/V_b$ and equation (8). The hot spot temperature comes from $R = V_c/V_d$.

For this mode of operation, all temperatures reported were from the trailing edge (Fig. 4). Background temperature and associated area are plotted in Fig. 9 for one test on Disk B1. The sampling rate was 100 Hz. It may be seen that the background signal variation is almost entirely due to growth of the radiating area. The background temperature is nearly constant at about 90°C from the time at which the area became large enough to measure a temperature. The areas seem reasonable since the area of the slider trailing edge in the field of view is 0.7 mm^2. Heating of adjacent disk material would account for the measurement of 1.5 mm^2. Some of the disk surface is in the field of view after leaving the contact. The sampling rate must be much greater to characterize a hot spot.

Table 1 contains data on thirty-nine hot spots observed during one test of Disk B1. Tabulated are the time at which the event occurred, the duration as measured at one-half of peak signal, the temperature and the area-both at peak signal. Sampling rate was 300 kHz. During this mode of operation, resolvable temperature events are occurring at the rate of about

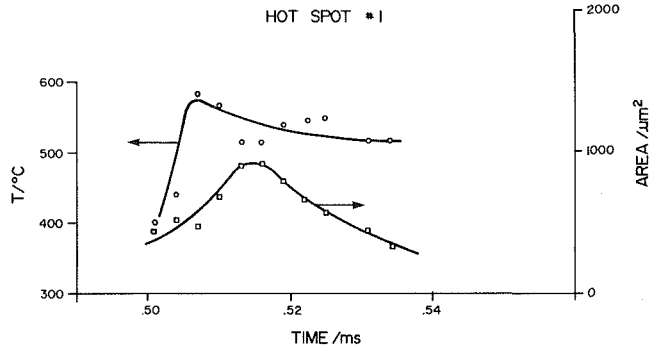

Fig. 10(*a*) Hotspot temperature and area versus time-mode III

Table 2 Hotspots Observed with Momentary Overload (V) and After Particle Contamination (IV)

Operating mode	Disk	Duration μs	Temperature °C	Area μm²
IV	B1	14	217	10,600
IV	B2	20	536	450
V	B1	21	360	1,200
V	B1	11	341	1,250
V	B1	15	464	420
V	B1	15	404	670
V	B1	27	366	710
V	B1	30	429	360
V	B1	20	421	470
V	B1	20	387	590
V	B2	25	364	970
V	B2	20	394	990
V	B2	25	382	730
V	B2	15	471	530
V	B2	27	488	380

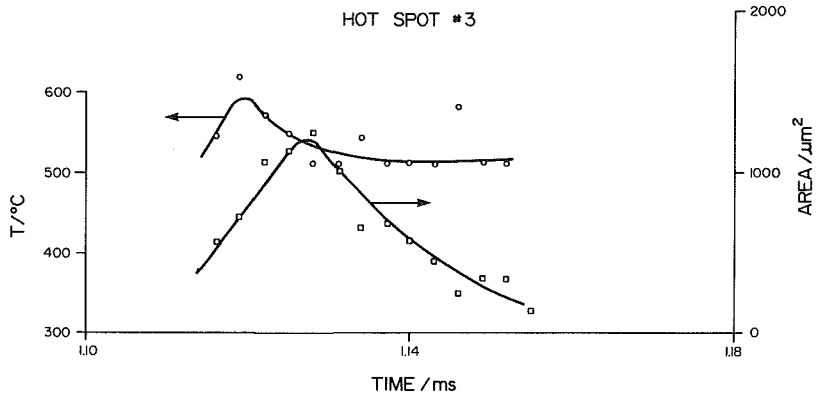

Fig. 10(*b*) Hotspot temperature and area versus time-mode III

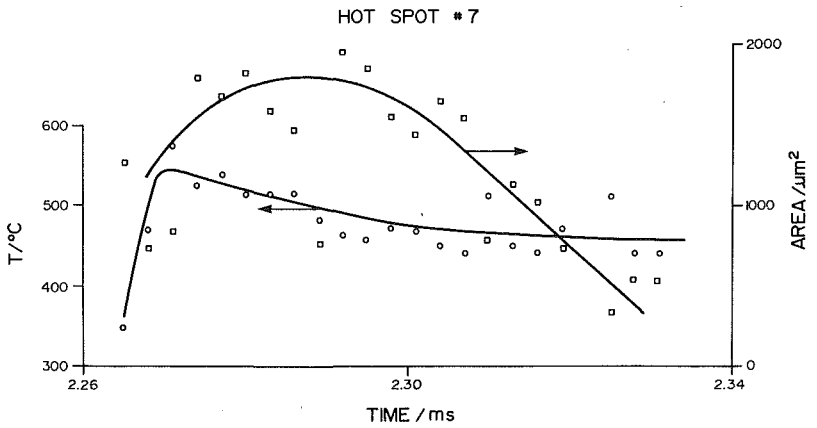

Fig. 10(*c*) Hotspot temperature and area versus time-mode III

2000 per second at the trailing edge of one rail of the slider. The time variation of three of the tabulated hot spots is exhibited in Figs. 10(*a–c*). There was severe damage to the disk surface in this mode. The base metal (aluminum) was eventually exposed.

4.1.2 Flying with Debris Particles. Whereas the continuous overload yields a great many hot spots per unit time, this is not a realistic occurrence with disk drives. Particle contamination of the disk surface may, however, occur. To simulate this mode of operation, alumina particles were poured on the moving disk surface ahead of the R/W head flying at standard load of 0.1 N. Particle sizes of 0.15, 15 and 50 μm were used. The two smaller particle sizes produced no detectable hot spots. The 50 μm particles produced the hot spots tabulated for peak signal conditions in Table 2. Sampling rate was 1 MHz. For this mode and the next all measurements were taken at the leading edge since no temperature events could be detected at the trailing edge. Resolvable events were rare in this mode—fewer than 10 per second. The time variation of temperature for two examples is shown in Fig. 11(*a–b*). The background temperature is essentially ambient in this mode. No detectable temperature events were observed for disk A. There was visible damage to the disk in this mode in the form of scratches in the direction of motion.

4.1.3 Flying After Momentary Overload. In order to simulate shock loading of the disk drive, a load of 1.8 N was applied for about 0.3 seconds after which the load returned to 0.1 N. Recording began after the load was reduced. This mode of operation produced temperature events which occurred in clusters with a rate of about 1000 hot spots per second during a cluster with quiescent intevals between. Temperature events could be detected for several seconds after the overload. The background temperature was nearly ambient. Some temperature events are tabulated in Table 2. Again, tabulated values are calculated from the peak signal levels. One hot spot is characterized in Fig. 12. No detectable events were observed for disk A. Surface damage to the disk was similar to the previous mode.

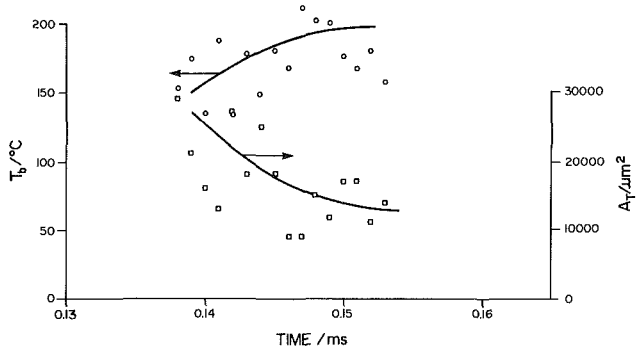

Fig. 11(*a*) Hotspot temperature and area-mode IV - disk B1

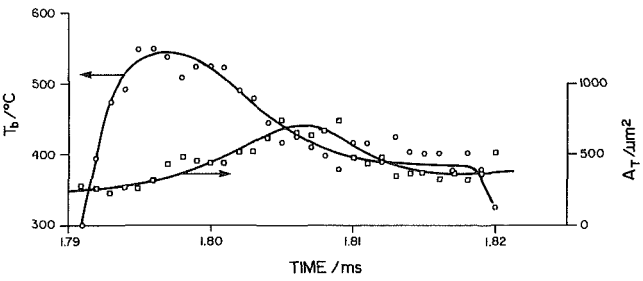

Fig. 11(*b*) Hotspot temperature and area-mode IV - disk B2

4.2 Friction Measurements. Friction force data was recorded during the Mode III operation (continuous overload). The force transmitted through the load lever (Fig. 5) produces a substantial zero offset in the friction force signal such that when an overload is applied, friction force readings are relative—not absolute. Relative friction force was recorded concurrently with detector output for Mode III. This force showed a nearly harmonic oscillation at 3 kHz and as such there was no apparent correlation with the very short duration (about 20 μs) hot spots. This is not surprising since the natural frequency of the head, suspension and elastic element in the frictional (tangential) direction is 526 Hz. The friction force measurement could not respond to an event as short in duration as the observed hot spots. The recorder used in Modes IV and V did not permit simultaneous friction measurement.

Friction force was measured in separate experiments for the standard load of 0.1 N for each type of disk. The friction during normal flying was too low to be resolved with this device. Coefficients of friction were measured for start-up (static friction) and flying with 50 μm alumina particles in the path. The results are listed in Table 3.

4.3 Air Film Thickness Measurements. The flying height or air film thickness during normal flying was measured using an optical interference technique. A vertical illumination microscope was positioned above the sapphire head. A narrow band-pass filter was installed in the light source. The filter band was centered at 605 nm. The movement of interference fringes indicates the separation of the surfaces as light is reflected from both the bottom of the head and the top of the disk. For a bright fringe the separation is

$$h_+ = \frac{\lambda}{2}(n+\phi)$$

and for a dark fringe

$$h_- = \frac{\lambda}{2}(n+\phi-\tfrac{1}{2})$$

if the separating medium has refractive index of one. Here, λ = 605 nm and, ϕ, the phase change on reflection was found to be zero. The order of the fringe is n.

Disk speed was controlled by manually braking the disk. Disk B2 was used. Speed was measured with an optical encoder.

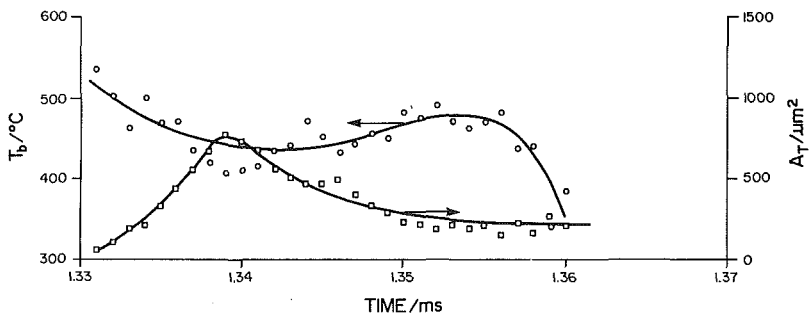

Fig. 12 Hotspot temperature and area-mode V - disk B2

Table 3 Friction coefficients 0.1 N load

Disk:	B2	B1	A
Static at start up	0.49	0.60	0.23
Flying with debris	0.26	0.26	0.44

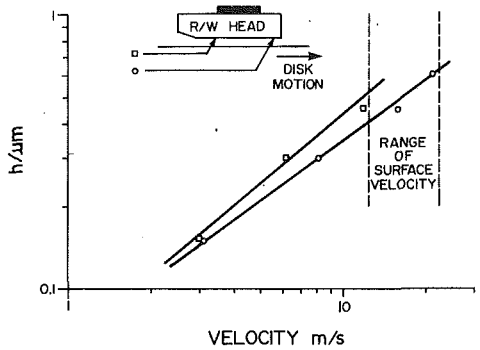

Fig. 13 Film thickness versus velocity

The results are shown in Fig. 13 for two locations—leading and trailing edge. Overloading the head with a 1.8 N load removed all apparent separation. Adding 50 μm particles to the path showed two effects. Particles would sometimes pile up at the front of the head. In the presence of the particles the head would at times lift up about 2 μm and remain lifted for several seconds. Perhaps the particles were entering and trapped in the wedge formed by the leading edge chamfer of the head and the disk surface.

When the disk surface was damaged, very small dark particles would lightly adhere to the head contact area. When the head was lifted the particles remained with the head as viewed through the microscope with monochromatic light. These dark particles were initially about 2 μm diameter. They would act as an attachment point for other particles so that the dark spot would grow toward the leading edge until about 25 μm wide and 200 μm long (in sliding direction). This took about 5 seconds. Now, if the disk was stopped, the running separation did not change. So, it can be assumed that this transferred material was about 0.5 μm thick (normal flying separation) and supported a portion of the load while running. The area of these spots is similar to the area of the measured hot spots. The life times associated with each are, however, very different.

5 Conclusions

An infrared temperature measurement system was designed and constructed which uses the spectral distribution as well as intensity of sampled radiation to determine both the temperature and effective area of a microscopic source at elevated temperature amid a low temperature background. This system was used to investigate hot spots occurring at the contact between a hard disk platter and a simulated R/W head made of IR transparent sapphire. Measurements were also made of friction coefficients and film thickness.

During normal flying and start/stop operations, no hot spots were detected but may be occurring outside the resolution limits of the system. When the head/disk contact was continuously overloaded, hot spots occurred at a high rate with temperatures of about 540°C, duration of 30μs, and areas of 1000 μm^2 being common. Particles of debris on the disk surface produced occasional 170 to 535°C spots of 360 to 15,000 μm^2 area and 5 to 20 μs duration. Flying after a momentary overload produced a high rate of hot spots for several seconds of the same character as the continuous overloading except that the temperatures were lower (360–490°C).

The normal flying separation of the head and disk was measured using optical interference to be at least 0.4 μm. Since this is much larger than the average roughness of the disk, hot spots are not expected. If the disk surface is damaged from overloading of the head/disk contact or from abrasive particle contamination an asperity of greater height than the head/disk separation may appear. For a surface velocity of 20 m/s, such an asperity would be in the IR detector view and in contact with the head for 30 μs or about the same as the duration of the observed hot spots.

The high temperatures of the hot spots and severe disk surface damage which occurred during continuous overloading were consistent with local melting of the disk substrate. The substrate was aluminum alloy (4 percent Mg) which has a melting temperature of 590°C.

The temperature data contained in this paper should not be used to discriminate among the disk types. Disk A had substantially lower emissivity than B1 and was less likely to produce enough radiation to detect a temperature event. Experimental effort was concentrated on disks with greatest likelihood of producing measurable results.

References

Bhushan, B., 1984, "Analysis of the Real Area of Contact Between a Polymeric Magnetic Medium and a Rigid Surface", ASME JOURNAL OF TRIBOLOGY, Vol. 106, No. 1, pp. 26–34.

Bhushan, B., 1985, "The Real Area of Contact in Polymeric Magnetic Media II: Experimental Data and Analysis," *ASLE Trans.*, Vol. 28, No. 2, pp. 181–197.

Bhushan, B., 1990, *Tribology and Mechanics of Magnetic Storage Devices*, Springer-Verlag, New York.

Bhushan B., Bair, S., Gulino, R., and Winer, W. O., 1985, "Infrared Measurement of Tape Surface Temperatures With a Simulated Head-Tape Interface," Tucson Technical Report TR-82.0132, IBM Corp. Tucson, Arizona, May 1985.

Bhushan, B., and Doerner, M. F., 1989, "Role of Mechanical Properties and Surface Texture In the Real Area of Contact of Magnetic Rigid Disks," ASME JOURNAL OF TRIBOLOGY, Vol. 111, pp. 452–458.

Gulino, R., Bair, S. Winer, W. O., and Bhushan, B., 1986, "Temperature Measurements of Microscopic Areas Within a Simulated Head/Tape Interface Using Infrared Radiometeric Technique," ASME JOURNAL OF TRIBOLOGY, Vol. 108, No. 1, pp. 29–34.

Weichart and Schonert, 1978, "Heat Generation at Tip of a Moving Crack," *J. Mech. Phys. Solids*, Vol. 26, pp. 151–161.